Supporting Information

Ternary platinum-copper-nickel nanoparticles anchored to hierarchical carbon supports as free-standing hydrogen evolution electrodes

Yi Shen*[1,2], Aik Chong Lua[2], Jingyu Xi*[3] and Xinping Qiu*[3,4]

[1] School of Food Science and Technology, South China University of Technology, Guangzhou, 510640, China. Tel. & Fax: +86 2087113843; email: feyshen@scut.edu.cn (Y. Shen)

[2] School of Mechanical and Aerospace Engineering, Nanyang Technological University, 50 Nanyang Avenue, 639798, Republic of Singapore. Tel.: +65 67905535.

[3] Institute of Green Chemistry and Energy, Graduate School at Shenzhen, Tsinghua University, Shenzhen 518055, China. Tel.:+86 75526036436; Fax: +86 75526036181; email: xijy@tsinghua.edu.cn (J. Xi)

[4] Key Lab of Organic Optoelectronics and Molecular Engineering, Department of Chemistry, Tsinghua University, Beijing 100084, China. Tel. & Fax: +86 1062794234; email: qiuxp@tsinghua.edu.cn (X. Qiu)

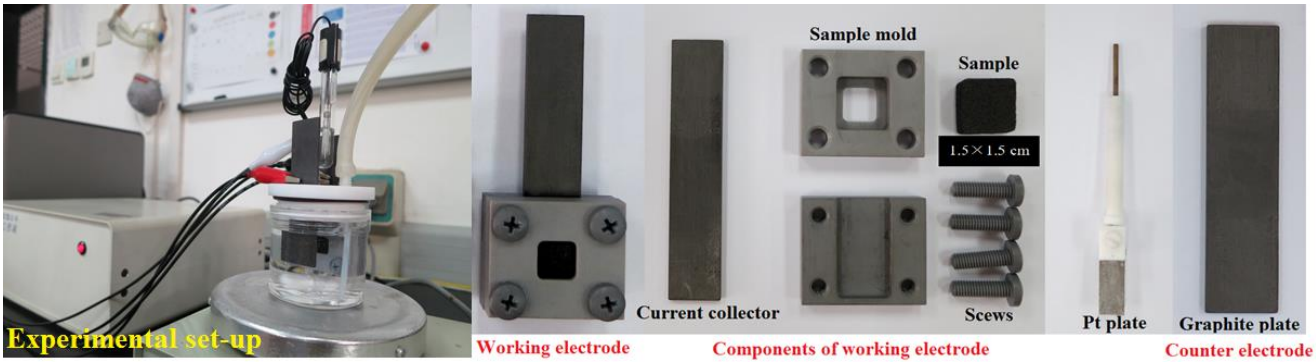

Figure S1 Experimental set-up of electrochemical measurements.

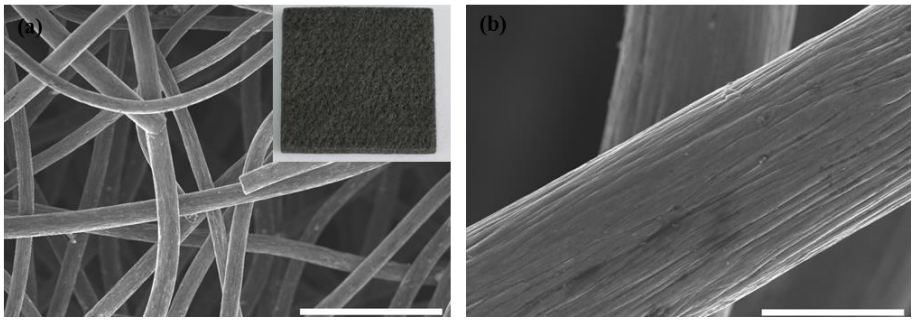

Figure S2 FESEM micrographs of pristine carbon felt (Inset in (a) is an optical image of a piece of 5 × 5 × 0.5 cm carbon felt sheet.) Scale bars, 100 μm (a), 10 μm (b)

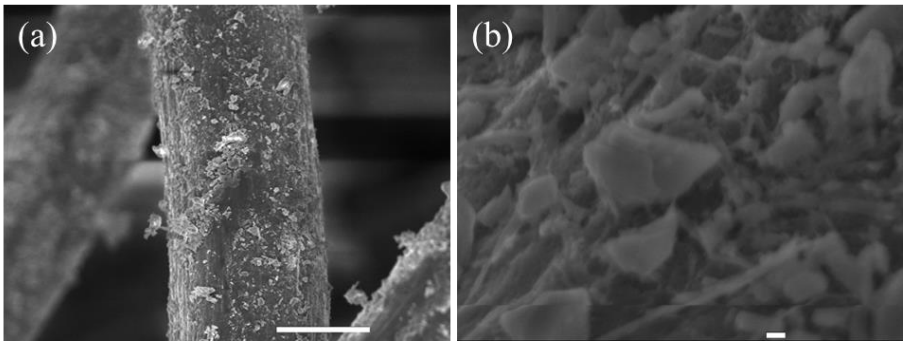

Figure S3 FESEM micrographs of nickel-copper oxalates decorated carbon felt. Scale bars, 10 μm (a), 100 nm (b).

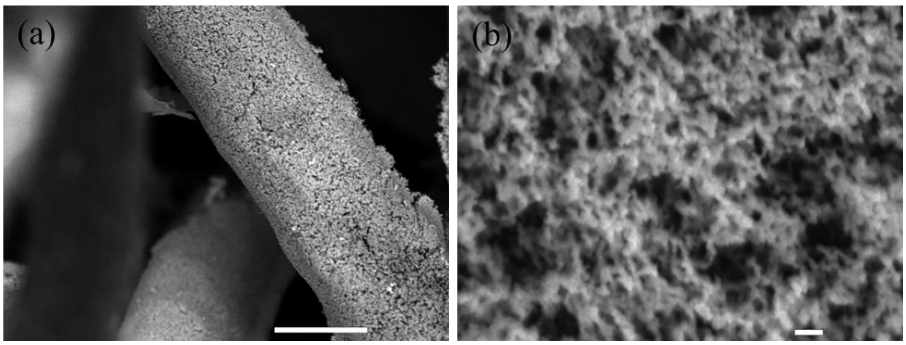

Figure S4 FESEM micrographs of metallic nickel-copper decorated carbon felt. Scale bars, 10 μm (a), 100 nm (b).

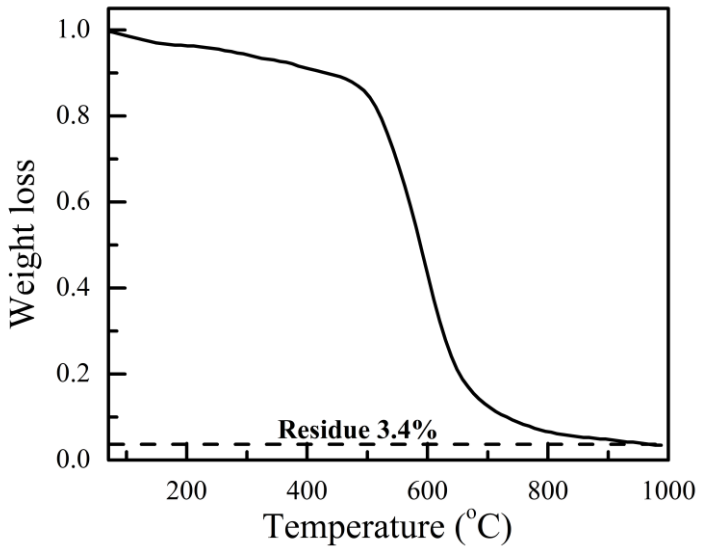

Figure S5 Thermogravimetric curves of $Pt_{42}Cu_{57}Ni_1$/CNF@CF.

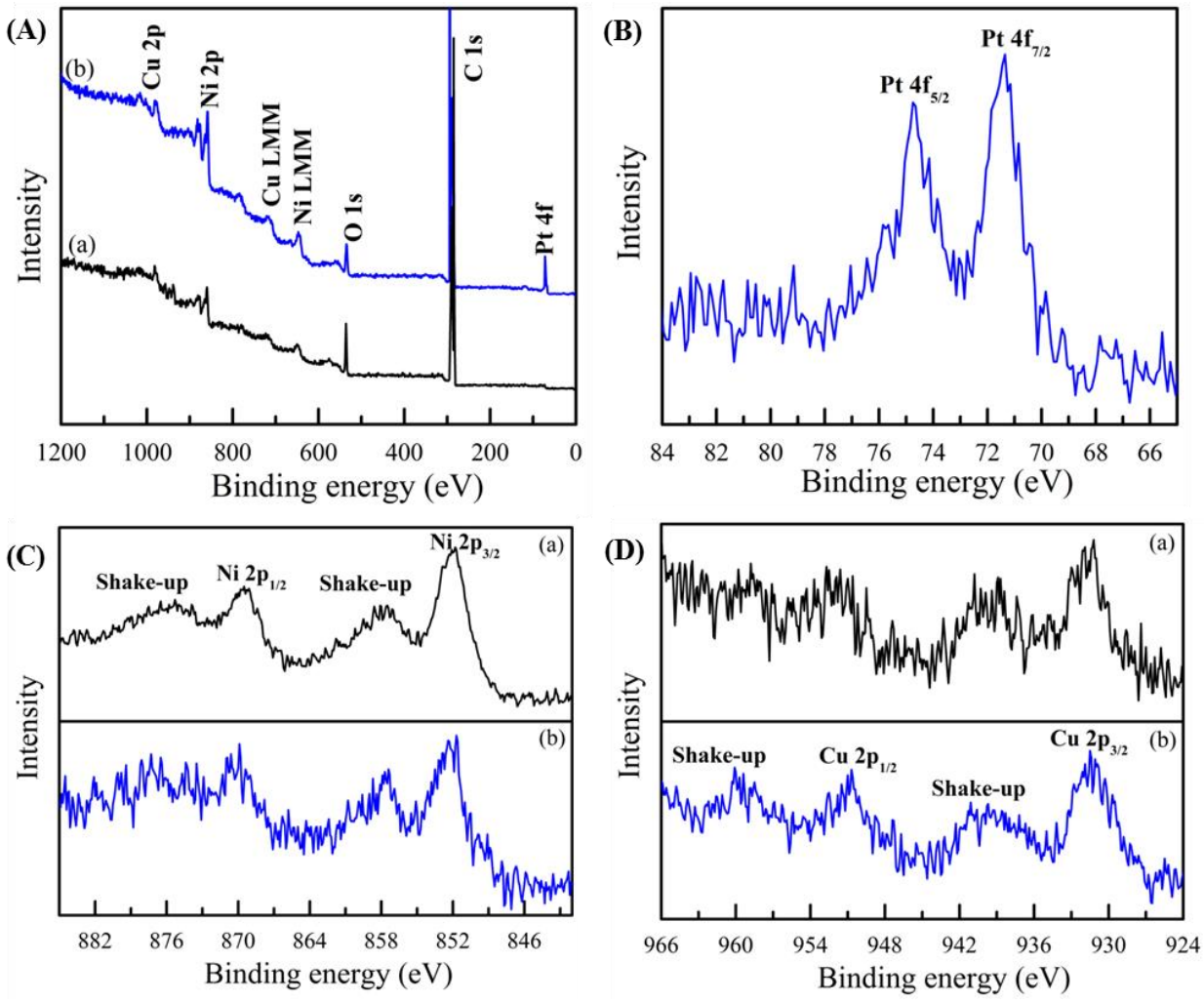

Figure S6 (A) Survey spectra, XPS profiles of (B) Pt 4f, (C) Ni 2p and (D) Cu 2p in (a) $Ni_{65}Cu_{35}$/CNF@CF and (b) $Pt_{13}Cu_{73}Ni_{14}$/CNF@CF

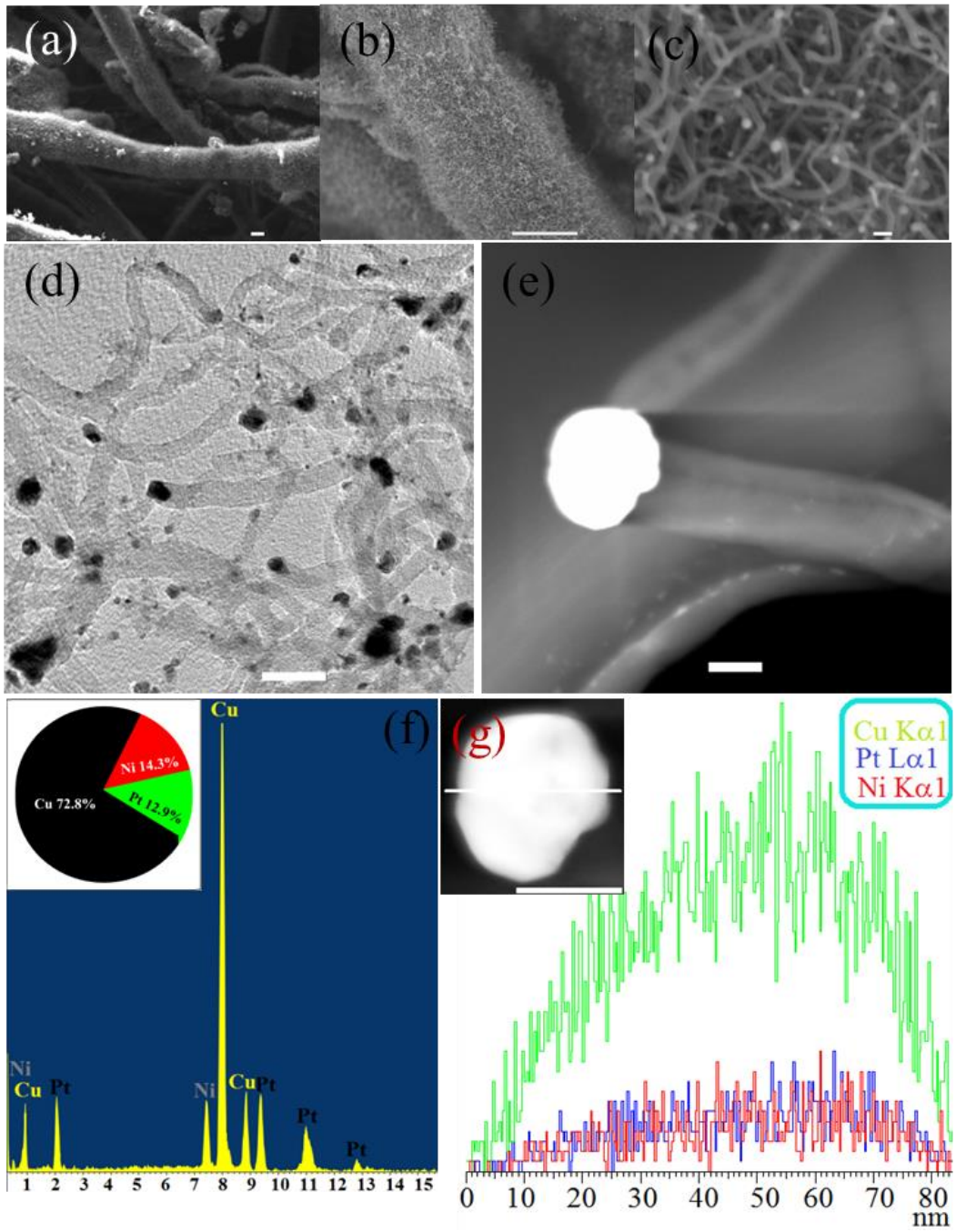

Figure S7 (a)-(c) FESEM micrographs of $Pt_{13}Cu_{73}Ni_{14}$/CNF@CF, (d) TEM, (e) HAADF-STEM micrographs of isolated $Pt_{13}Cu_{73}Ni_{14}$/CNF@CF, (f) EDS profile of $Pt_{13}Cu_{73}Ni_{14}$ NPs (inset in (f), atomic composition of $Pt_{13}Cu_{73}Ni_{14}$ NPs), (g) line scan and elemental distribution of a $Pt_{13}Cu_{73}Ni_{14}$ NP. Scale bars, 10 µm (a, b), 100 nm (c), 200 nm (d), 50 nm (e) and (g)

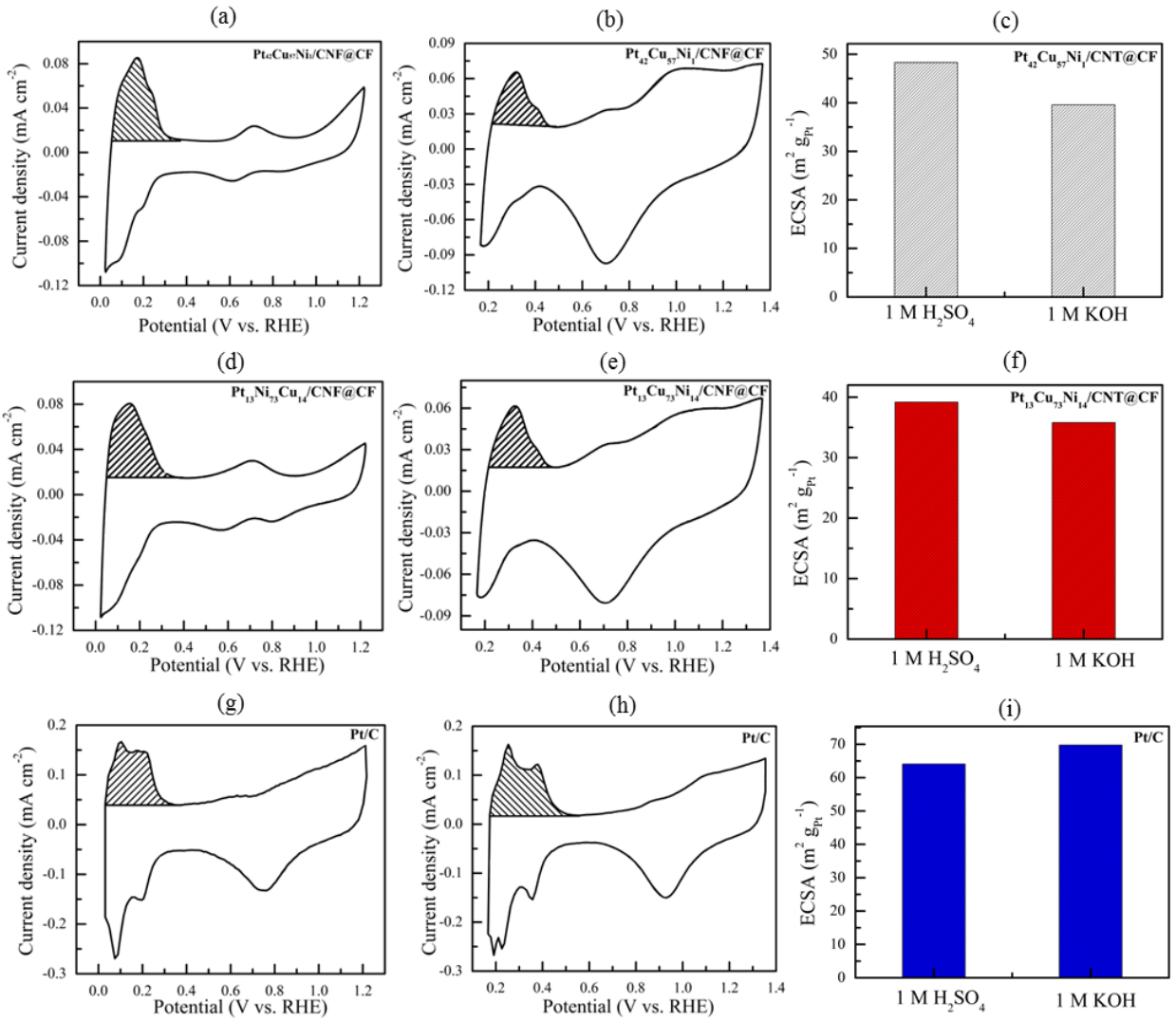

Figure S8 (a) and (b) Cyclic voltammetry curves of $Pt_{42}Cu_{57}Ni_1$/CNF@CF in 1 M H_2SO_4 and 1 M KOH with a can rate of 50 mV s^{-1}, respectively, and (c) ECSA values of $Pt_{42}Cu_{57}Ni_1$/CNF@CF in 1 M H_2SO_4 and 1 M KOH; (d) and (e) cyclic voltammetry curves of $Pt_{13}Cu_{73}Ni_{14}$/CNF@CF in 1 M H_2SO_4 and 1 M KOH with a can rate of 50 mV s^{-1}, respectively, and (f) ECSA values of $Pt_{13}Cu_{73}Ni_{14}$/CNF@CF in 1 M H_2SO_4 and 1 M KOH; (g) and (h) cyclic voltammetry curves of Pt/C in 1 M H_2SO_4 and 1 M KOH with a can rate of 50 mV s^{-1}, respectively, and (i) ECSA values of Pt/C in 1 M H_2SO_4 and 1 M KOH.

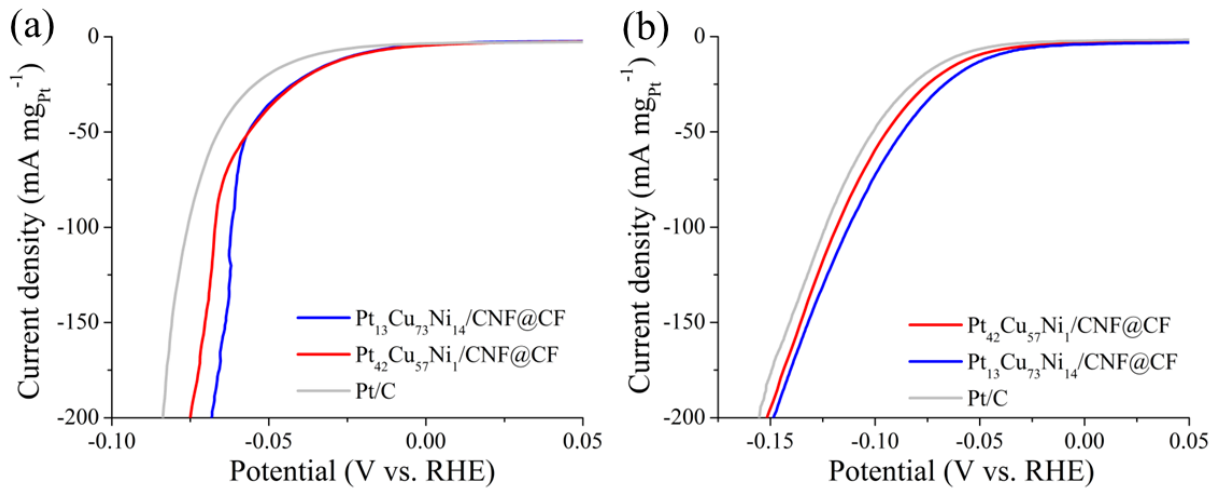

Figure S9 (a) and (b) Pt-mass normalized polarization curves of catalysts in 1 M H_2SO_4 and 1 M KOH, respectively.

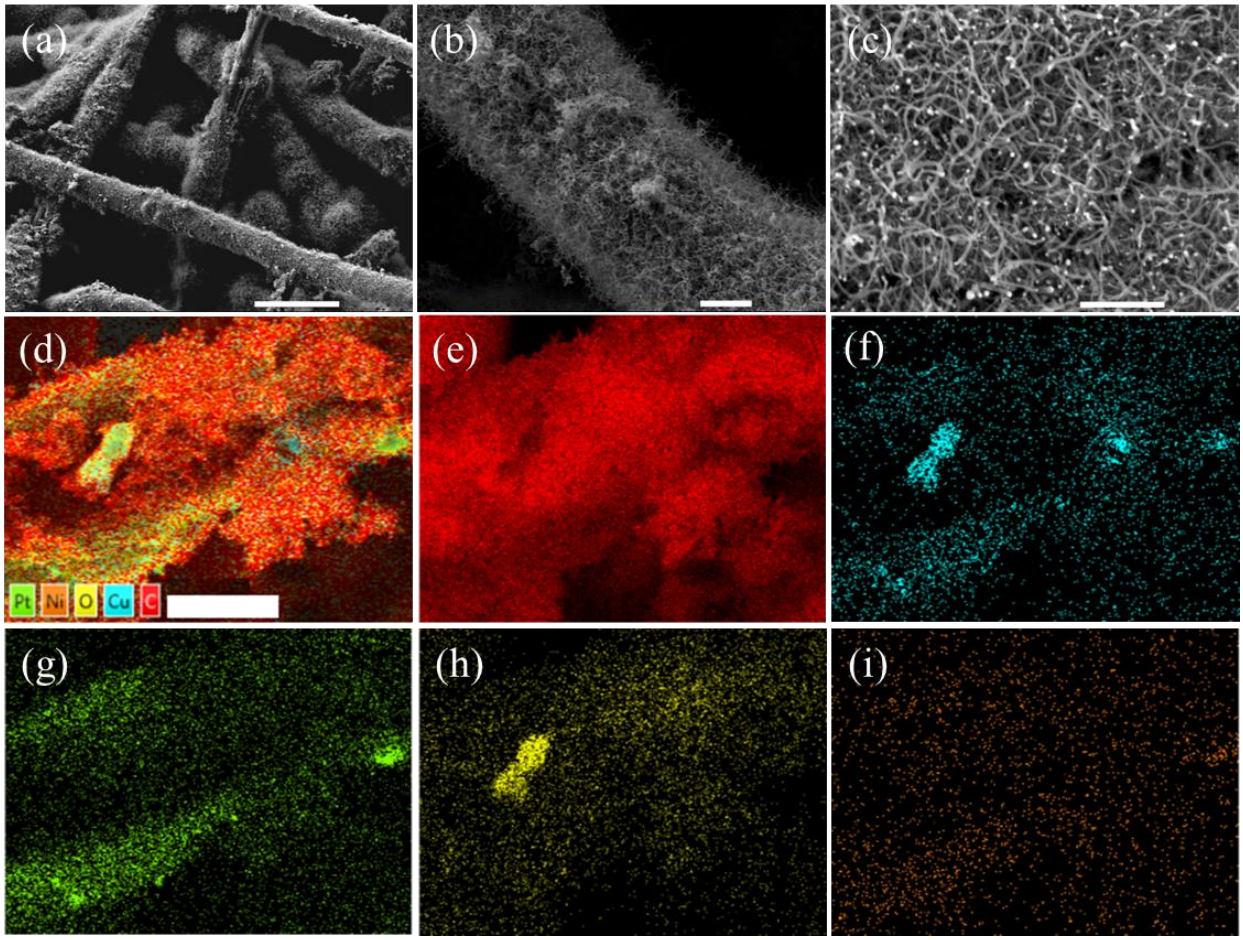

Figure S10 (a)-(c) FESEM micrographs of spent $Pt_{13}Cu_{73}Ni_{14}$/CNF@CF in 1 M H_2SO_4, (d) overall EDS micrograph, (e)-(i) elemental mapping micrographs of carbon, copper, platinum, oxygen, and nickel, respectively. Scale bar, 10 μm.

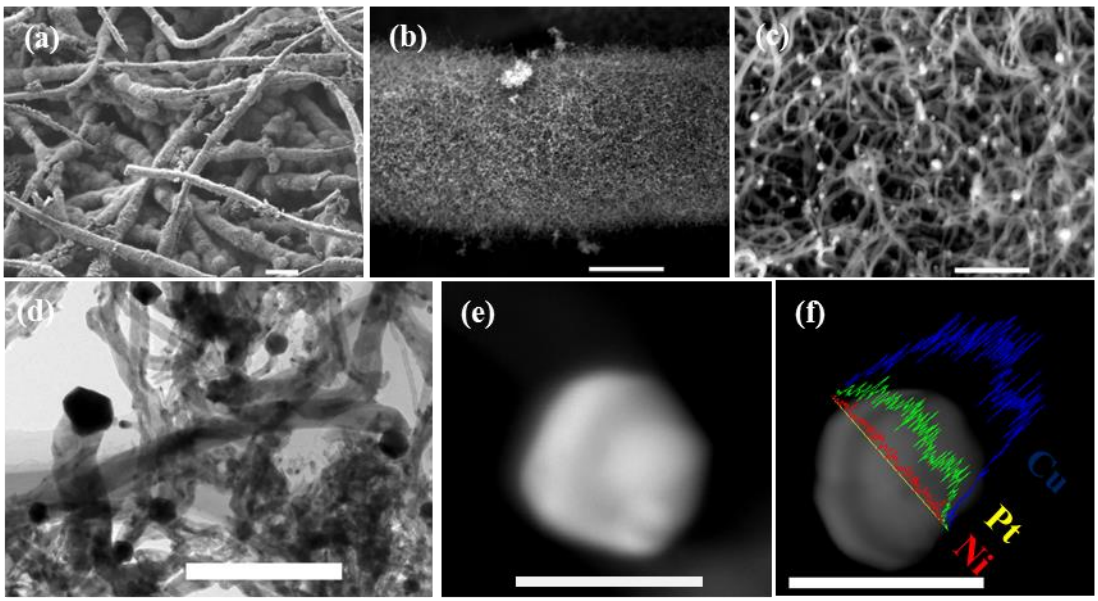

Figure S11 (a)-(c) FESEM micrographs of spent $Pt_{42}Cu_{57}Ni_1$/CNF@CF in 1 M H_2SO_4, (d) TEM micrograph of isolated $Pt_{42}Cu_{57}Ni_1$/CNF@CF, (e) high-resolution HAADF-STEM micrograph of a typical $Pt_{42}Cu_{57}Ni_1$ NP, (f) line scan and elemental distribution of a $Pt_{42}Cu_{57}Ni_1$ NP. Scale bars, 100 µm (a), 10 µm (b), 1 µm (c) and (d), 100 nm (e) and (f)